Materials Chemistry and Physics 171 (2016) 281–289

Contents lists available at ScienceDirect

Materials Chemistry and Physics

journal homepage: www.elsevier.com/locate/matchemphys

Polystyrene/silica microspheres with core/shell structure as support of tungstophosphoric acid

Marina N. Gorsd**, Mirta N. Blanco, Luis R. Pizzio*

Centro de Investigación y Desarrollo en Ciencias Aplicadas "Dr. J.J Ronco" (CINDECA), Departamento de Química, Facultad de Ciencias Exactas, UNLP-CCT La Plata, CONICET, 47 N° 257, 1900 La Plata, Argentina

HIGHLIGHTS

- Tungstophosphoric acid on core/shell polystyrene/silica microspheres were prepared.
- Spheres presented a narrow size distribution and SiO_2 nanoparticles uniform layer.
- Mesoporous tungstophosphoric acid impregnated solids were achieved.
- Tungstophosphate anion with undegraded Keggin structure is present in the solids.
- Solids have very strong acid sites being suitable for use in acid catalyzed reactions.

GRAPHICAL ABSTRACT

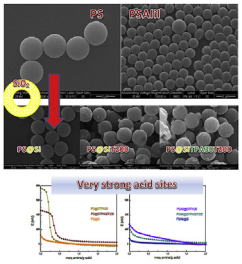

ARTICLE INFO

Article history:
Received 22 August 2015
Received in revised form
16 November 2015
Accepted 4 January 2016
Available online 9 January 2016

Keywords:
Composite materials
Sol–gel growth
Electron microscopy
Nuclear magnetic resonance

ABSTRACT

The immobilization of tungstophosphoric acid (TPA) on polystyrene/silica microspheres with core/shell structure by the incipient wetness impregnation technique was studied. The materials were synthesized employing polystyrene (PS) spheres or polystyrene spheres with the addition of 3-amino-1-propene as core, which were coated with silica by a modified Stöber method, using tetraethylorthosilicate as precursor. Spheres with a narrow size distribution and a uniform layer formed by silica nanoparticles were obtained, as observed by SEM and TEM. After impregnation with TPA, the samples were calcined at 200 °C in order to obtain the final materials. The solids impregnated with TPA presented N_2 adsorption –desorption isotherms characteristic of mesoporous materials. In addition, the characterization by FT-IR and ^{31}P NMR of all the solids impregnated with TPA gave evidence of the presence of the tungstophosphate anion with Keggin structure, and by potentiometric titration it was estimated that the solids present very strong acid sites. So, they are good candidates to be used in reactions catalyzed by acids, specifically for imidazole synthesis.

1. Introduction

Nanosized materials of the core/shell type have become very important due to their high functionality and properties, which can be easily modified by changing either the composition of the materials they contain or their core/shell ratio [1].

The combination of the materials employed in their synthesis

* Corresponding author.
** Corresponding author.
E-mail addresses: marinagorsd@conicet.gov.ar (M.N. Gorsd), lrpizzio@quimica.unlp.edu.ar (L.R. Pizzio).

http://dx.doi.org/10.1016/j.matchemphys.2016.01.019
0254-0584/

can vary widely. Polymer microspheres such as polystyrene (PS) and poly(methyl methacrylate) (PMMA) and silica microspheres are often used as core spheres, and metal nanoparticles or oxide nanoparticles as shells [2]. The composites can include both inorganic cores and shells such as SiO_2/TiO_2 or ZnO/TiO_2, as well as an inorganic/organic core/shell such as Zr/PMMA or TiO_2/PS, or organic/inorganic core/shell such as PS/SiO_2 or PS/TiO_2. The choice of the core and the shell solely depends on the application that will be given to each material [3]. A nice and comprehensive review of these types of solids was recently reported by Chaudhuri and Paria [4].

A two-step process is usually used to prepare core/shell particles. Firstly, the core particles are obtained and afterwards, the precursor material of the shell is deposited on the core particles. This procedure is done by different methods, according to the core and the shell materials [4]. Core/shell microspheres with a solid core and a porous silica shell have been increasingly used, e.g., for efficient separations, catalysis, and biomedical applications [2,5–7]. The silica coating is usually deposited on polymer microspheres.

The material behavior is notably influenced by the particle size and the shell thickness [8]. It can be remarked that a small width of the porous shell is an advantage as the diffusion path length is short, so giving faster mass transfer in both packed separation columns [9] and catalytic reactions, because the entry, the transport and the release of different substances are facilitated [10].

Some of these materials are used for the production of hollow solids, through the application of a sacrificial core technique. When an organic core is used, it is removed by dissolution with a suitable solvent or by calcination [11,12]; instead, for the inorganic cores, dissolution by acids or bases is used [13,14].

Previous work has shown that the tungstophosphoric acid (TPA) can be supported on diverse materials, obtaining suitable materials for use as catalyst in reactions heterogeneously catalyzed by acids [15–20].

The heteropolyacids have special properties that make them particularly valuable for catalysis. Among them, their high Brønsted acidity, high solubility in water and oxygenated solvents, as well as an interesting stability when supported on different oxides and polymers can be highlighted. The last property is highly important, as the heteropolyacids present low specific surface area when they are employed in their bulk structure [21,22], while it considerably increases when they are supported.

In the present work the synthesis and characterization of solid acid catalysts, prepared using core/shell spheres of polystyrene/mesoporous silica as support, and impregnated with tungstophosphoric acid (TPA) employing the incipient wetness impregnation technique, are presented. Polystyrene spheres or polystyrene modified by the addition of a comonomer (allylamine) were used as core for the preparation of the support. These cores were covered with silica using a modified Stöber method [23], by means of hydrolysis and condensation of tetraethylorthosilicate (TEOS) in an ethanol–water solution using ammonium hydroxide as catalyst of the sol–gel reaction. Finally, the carriers were impregnated with TPA and then calcined. All the solids were characterized by different physicochemical techniques in order to observe the influence of the different preparation conditions on the characteristics of the synthesized materials, which were prepared to be later used as catalysts in an acid-catalyzed reaction.

2. Materials and methods

2.1. Preparation of polystyrene and allylamine added polystyrene cores

The polystyrene (PS) spheres were obtained employing the best conditions found in previous work [24]. They were prepared from 10 g of styrene utilizing 0.1 g of 4,4′ azobis 4-cyanovaleric acid (ACVA) as polymerization initiator in the presence of 0.3 g of polyvinylpyrrolidone (PVP) as stabilization agent of the dispersion, using ethanol as solvent. The mixture was placed in a 250 cm^3 reactor equipped with a reflux condenser, a temperature controller and a magnetic stirrer. N_2 was bubbled for 15 min in order to remove oxygen from the reactor. The temperature of the system was raised up to 70 °C and then the initiator, dissolved in a small quantity of ethanol, was added. The polymerization was carried out by stirring at 300 rpm for 24 h. After this time, the latex spheres were washed with ethanol to remove any remains of surfactant agent and then, they were stored dispersed in ethanol.

Following the same synthesis operative procedure, PS spheres with the addition of 1 cm^3 of 3-amino-1-propene (allylamine) as comonomer were prepared, thus obtaining the PSAlil material.

2.2. Preparation of silica-coated PS and PSAlil

To obtain the silica coating, PS spheres or PSAlil spheres, in a quantity of 60% w/w with respect to the silica quantity to be prepared, were weighed and placed in 40 cm^3 of ethanol and were then sonicated for 10 min in order to obtain a homogeneous dispersion. A modified version of Stöber method [23] was used for silica synthesis, which proceeds via hydrolysis/condensation of tetraethylorthosilicate (TEOS) in an alcohol/ammonium hydroxide reaction medium. Seven cm^3 of TEOS as silica precursor and 1 cm^3 of ammonium hydroxide (28% w/w) as catalyst of the sol–gel reaction were employed. The condensation reaction was performed at 50 °C with constant stirring for 20 h.

After this time, the coated spheres were separated by centrifugation and repeatedly washed with distilled water to remove the catalyst remains. Finally, they were dried at room temperature and then placed in a stove at 60 °C for 24 h, thus obtaining the solids that will be named PS@Si and PSAlil@Si.

2.3. Preparation of core/shell spheres with tungstophosphoric acid

Employing the incipient wetness impregnation technique and using a 30% (w/w) solution of tungstophosphoric acid ($H_3PW_{12}O_{40}.23H_2O$) (TPA) in ethanol–water (1:1 v/v), the following materials were impregnated: latex spheres with and without allylamine addition coated with silica (PS@Si) and (PSAlil@Si). The quantity of TPA solution was fixed in order to obtain 30% TPA w/w in the final material. The system was kept at room temperature till complete dryness. Afterward, the obtained solids (PS@SiTPA30 and PSAlil@SiTPA30) were weighed. Besides, the quantity of non-impregnated TPA in the washings with ethanol from the vessel where the impregnation was carried out was quantified by atomic absorption spectrometry. These materials were then calcined at 200 °C to obtain the spheres that will be named PS@SiTPA30T200 and PSAlil@SiTPA30T200. The nomenclature of the prepared solids is summarized in Table 1.

Table 1
Solid nomenclature.

Support	Solid impregnated with 30% TPA	Solid calcined at 200 °C
PS@Si	PS@SiTPA30	PS@SiTPA30T200
PSAlil@Si	PSAlil@SiTPA30	PSAlil@SiTPA30T200

2.4. Characterization

2.4.1. Atomic absorption spectrometry

The TPA quantitative determination was performed on the above-mentioned washings. Tungsten concentration values in solution were obtained using the calibration curve method. The curve was set up utilizing tungsten standards prepared in the laboratory from sodium tungstate ($Na_2WO_4.2H_2O$) within the concentration range that corresponds to a linear absorbance response as a function of the concentration (50–500 ppm of W). Standards of 50, 100, 200, 300, 400 and 500 ppm of W were hence employed for the calibration curve. The different solutions were measured with a Varian double beam spectrophotometer model SpectrAA 240, using a tungsten hollow monocathode lamp. The analysis was carried out at a wavelength of 251.1 nm, a slit of 0.2 nm, a current lamp of 15 mA, and an acetylene–nitrous oxide flame ratio of 11:14.

2.4.2. Scanning electron microscopy

The morphological study of all the solids (PS@Si, PS@SiTPA30, PS@SiTPA30T200, PSAlil@Si, PSAlil@SiTPA30, PSAlil@SiTPA30T200 samples) and tungsten distribution on the solids were studied by scanning electron microscopy (SEM), using Philips equipment, model 505, at a working potential of 15 kV. The samples were supported on graphite and metallized with a sputtered gold film before the measurement.

The mean sphere diameter of PS and its distribution were obtained from the SEM images of the samples, using ADDAII acquisition device, with Soft Imaging System, at a magnification of 10000×, measuring a few hundred spheres.

2.4.3. Transmission electron microscopy

The solids were studied by transmission electron microscopy (TEM) in a JEOL 100 CXII microscope, working at 100 kV and at a magnification of 100000×. The samples were crushed in an agate mortar, ultrasonically dispersed in isobutanol, and deposited on a carbon-coated copper grid.

2.4.4. Fourier transform infrared spectroscopy

The Fourier transform infrared (FT-IR) spectra of the solids were recorded with Bruker IFS 66 equipment. Pellets of ca. 1% w/w of the sample in KBr were prepared in a self-made device. A wavenumber range of 400–4000 cm^{-1} was studied, the resolution being 2 cm^{-1}.

2.4.5. N_2 adsorption–desorption at the liquid-nitrogen temperature

The specific surface area, the pore volume and the mean pore diameter of the solids were determined from the N_2 adsorption–desorption isotherms at the liquid-nitrogen temperature, obtained using Micromeritics Asap 2020 equipment. The solids were previously degassed at 100 °C for 2 h.

2.4.6. Potentiometric titration with n-butylamine

Potentiometric titration was used to evaluate the acidic characteristics of the solids. To this end, 50 mg of solid suspended in 45 cm^3 acetonitrile was stirred for 3 h. Then, the titration was carried out with a solution of n-butylamine in acetonitrile (0.05 N) at a flow rate of 0.05 cm^3/min. The electrode potential variation was measured in a Hanna 211 digital pH meter with a double-junction electrode.

2.4.7. Nuclear magnetic resonance spectroscopy

The solids impregnated with TPA, before and after being calcined at 200 °C, were analyzed by ^{31}P magic angle spinning-nuclear magnetic resonance (MAS–NMR) spectroscopy. For this purpose, Bruker MSL-300 equipment was employed, using 5 m pulses, a repetition time of 3 s, and working at a frequency of 121.496 MHz for ^{31}P at room temperature, the resolution being 3.052 Hz per point. A 5 mm diameter and 10 mm high sample holder was used, the spin rate was 2.1 kHz. Several hundred pulse responses were collected. Phosphoric acid 85% was employed as external reference.

2.4.8. X-ray diffraction

The X-ray diffraction (XRD) patterns were obtained by the Debye–Scherrer method (powder method). The patterns were recorded using Philips PW-1732 equipment with built-in recorder. The conditions used were: Cu Kα radiation, Ni filter, 20 mA and 40 kV in the high voltage source, scanning range from 5 to 60 °2θ, and a scanning speed of 1°/min.

3. Results and discussion

The incorporated TPA amount in the samples after impregnation (C_{FIN}), expressed as % TPA (w/w), was calculated by performing a mass balance between the $H_3PW_{12}O_{40}$ amount contained in the solution used for impregnation (C_{INI}) and the non-impregnated TPA amount (C_{REM}) remaining in the equipment used for impregnation. This amount was estimated from the measurement of the W concentration in the solution obtained by washing the impregnation equipment with distilled water. The corresponding TPA values are indicated in Table 2.

The TPA amount in the final material was determined by the following expression:

$$C_{FIN}\ (\%\ TPA(w/w)) = 100\ [C_{INI}\ (mg\ TPA) - C_{REM}\ (mg\ W)\ (TPA\ molecular\ weight/12\ W\ molecular\ weight)]/(support\ mass + TPA\ mass)$$

As shown in Table 2, practically all the TPA amount in the initial solution is actually impregnated in the support; only a small fraction of the initial TPA content remained in the container employed for impregnation.

The micrographs obtained by SEM of the PS and the PSAlil spheres are shown in Fig. 1. It can be observed that the core presents a uniform size of 2.5 μm diameter for the PS spheres without comonomer addition and 1 μm diameter for the PS spheres with allylamine addition. All the spheres are well dispersed without being agglomerated between them, suggesting that PVP is an excellent dispersion stabilizer agent [25].

The main purpose of the 3-amino-1-propene addition is to modify the surface: the amine group of the comonomer could cover the PS spheres with positive charge. Based on the report by Zou et al. [26], it can be assumed that such modification is an important factor for the optimization of the core coating. In the particular case of the spheres synthesized in the present work for their use as core for silica coating, it is considered that an acid–base interaction between the hydroxyl groups of the silica and the amine groups on the core surface would be generated.

On the other hand, the micrographs of the PS spheres covered with silica are presented in Fig. 2a. Here the absence of detached silica or silica forming amorphous aggregates becomes apparent, due to a previous optimization of the conditions needed for obtaining the covering [27].

In Fig. 2b and c, the micrographs of the PS spheres coated with silica and impregnated with tungstophosphoric acid, dried and calcined at 200 °C, respectively, are shown. It can be observed that the silica coating has a smooth and uniform appearance, and remains intact after calcination.

Similar results were observed for the PS spheres prepared with allylamine addition and then covered with silica and impregnated with TPA.

Table 2
Theoretical and measured TPA concentration.

Sample	Theoretical TPA concentration (% (w/w))	C_{INI} (mg TPA)	C_{REM} scanning electron microscopy (mg TPA)	C_{FIN} (% (w/w))
PS@SiTPA30	30	527.5	16.5	26.8
PSAlil@SiTPA30	30	121.4	24.8	28.1

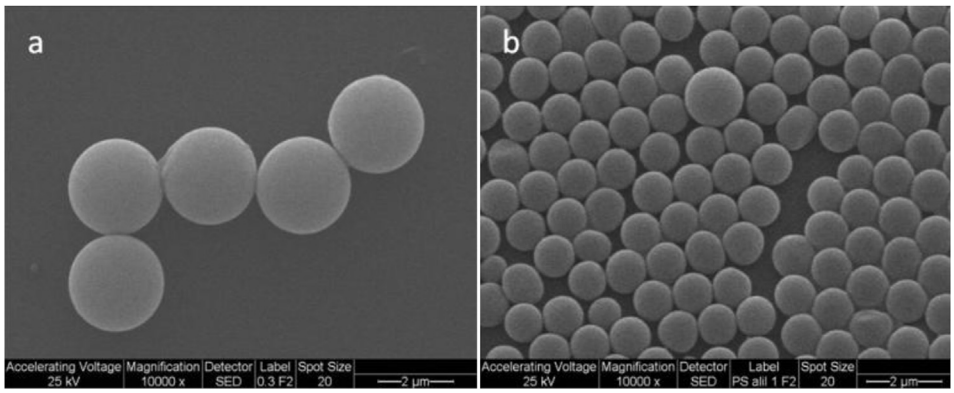

Fig. 1. SEM micrographs of (a) polystyrene spheres, (b) polystyrene spheres synthesized with 3-amino-1-propene addition. Magnification: 10000×, bar: 2 µm.

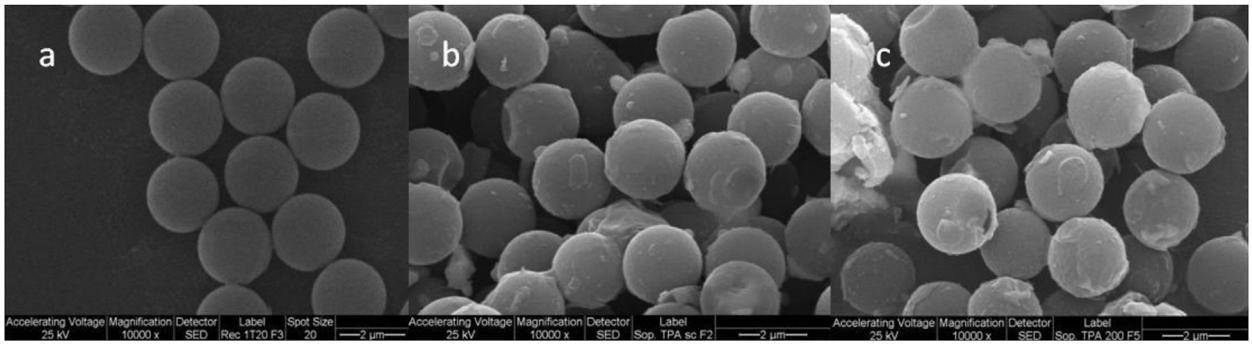

Fig. 2. SEM micrographs of (a) polystyrene spheres covered with silica, (b) silica-covered spheres impregnated with TPA, (c) silica-covered spheres impregnated with TPA after calcination at 200 °C. Magnification: 10000×, bar: 2 µm.

A regular and uniform layer formed by silica nanoparticles can be observed in the TEM micrographs (Fig. 3) of silica-covered PS spheres (PS@Si sample), silica-covered PS spheres calcined at 200 °C (PS@SiT200 sample), and silica-covered spheres impregnated with TPA and then calcined at 200 °C (PS@SiTPA30T200 sample). The thickness of the silica layer estimated for the PS@Si and PS@SiT200 based materials by this technique are around 100 nm. No significantly changes were detected as result of the TPA incorporation. Similar values were obtained for the PSAlil@ based materials.

The thickness of the silica layer estimated using the method reported by Zhang et al. [28] for the PS@Si and PSAlil@Si samples were somewhat lower (80 nm and 92 nm respectively).

The FT-IR spectrum of the synthesized polystyrene and that of the PS prepared with allylamine addition are presented in Fig. 4.

For polystyrene without comonomer addition (Fig. 4a), the

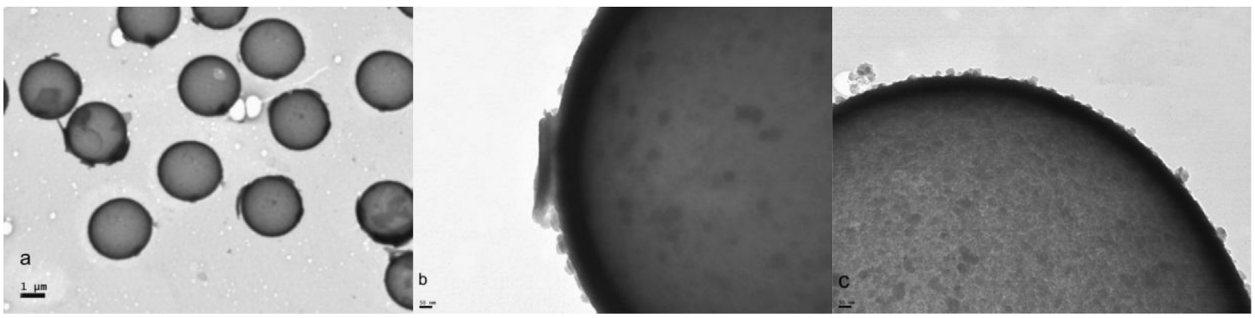

Fig. 3. TEM micrographs of (a) silica-covered PS spheres (PS@Si), (b) silica-covered PS spheres calcined at 200 °C (PS@SiT200), (c) silica-covered spheres impregnated with TPA after calcination at 200 °C (PS@SiTPA30T200). Magnification: 5000×, 10000×, and 10000×, respectively.

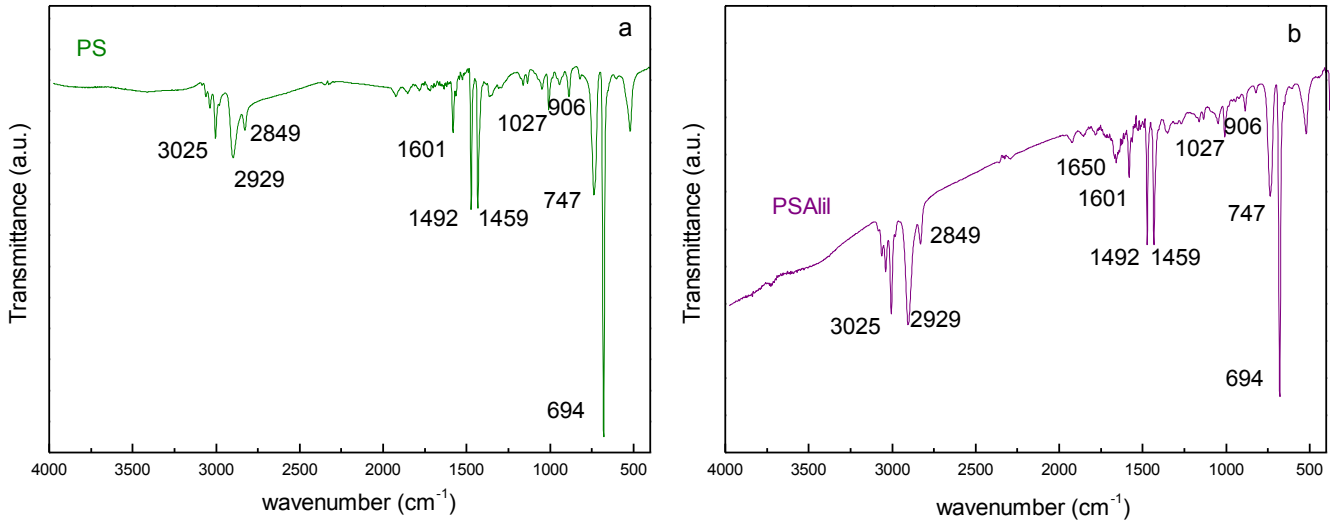

Fig. 4. FT-IR spectra of (a) PS spheres, (b) PS spheres with allylamine addition (PSAlil).

characteristic bands of PS such as the stretching vibration of the aromatic C–H bonds, the asymmetric stretching vibration of the C–H bonds corresponding to the CH_2 of the polystyrene backbone, and the stretching vibration of the aromatic ring C–C bonds are observed. In addition, the stretching and torsion vibrations of the C–H bonds belonging to the aromatic ring in or out the plane appear at 1459, 1027, 906, 747, and 694 cm^{-1}. These results are in good agreement with those reported in the literature [27,29].

In the spectrum shown in Fig. 4b, corresponding to the PSAlil sample, the same polystyrene characteristic bands such as those observed for the PS spheres appear. Additionally, the bands corresponding to the stretching vibration of the C=C bond and the amine group appear as a low intensity band placed at 1650 cm^{-1} and two very weak signals at 1150 and 1120 cm^{-1} respectively [29].

For the materials prepared with PS covered with silica, and impregnated with tungstophosphoric acid, the spectra presented in Fig. 5a were obtained. In those spectra the aforementioned bands belonging to PS were observed, and the characteristic bands of silica with maxima at 1104, 971 and 809 cm^{-1} appear, which are assigned to the stretching vibration of the Si–O–Si and Si–O groups, while the band at 470 cm^{-1} corresponds to the torsion vibration of the Si–O group, which agrees well with those reported in the literature [15].

In addition, the characteristic bands of the TPA assigned to the vibration of the P–Oa and W–Od bonds are displayed at 1080, and 981 cm^{-1}, respectively. Both appear as narrow bands superimposed to the bands corresponding to the Si–O groups of silica. The band assigned to the W–Ob–W bond placed at 894 cm^{-1}, is observed without overlapping.

On the other hand, the bands corresponding to the stretching vibration of the W–Oc–W bond and the bending vibration of the Oa–P–Oa bond appear at 794 and 594 cm^{-1}, respectively, which is

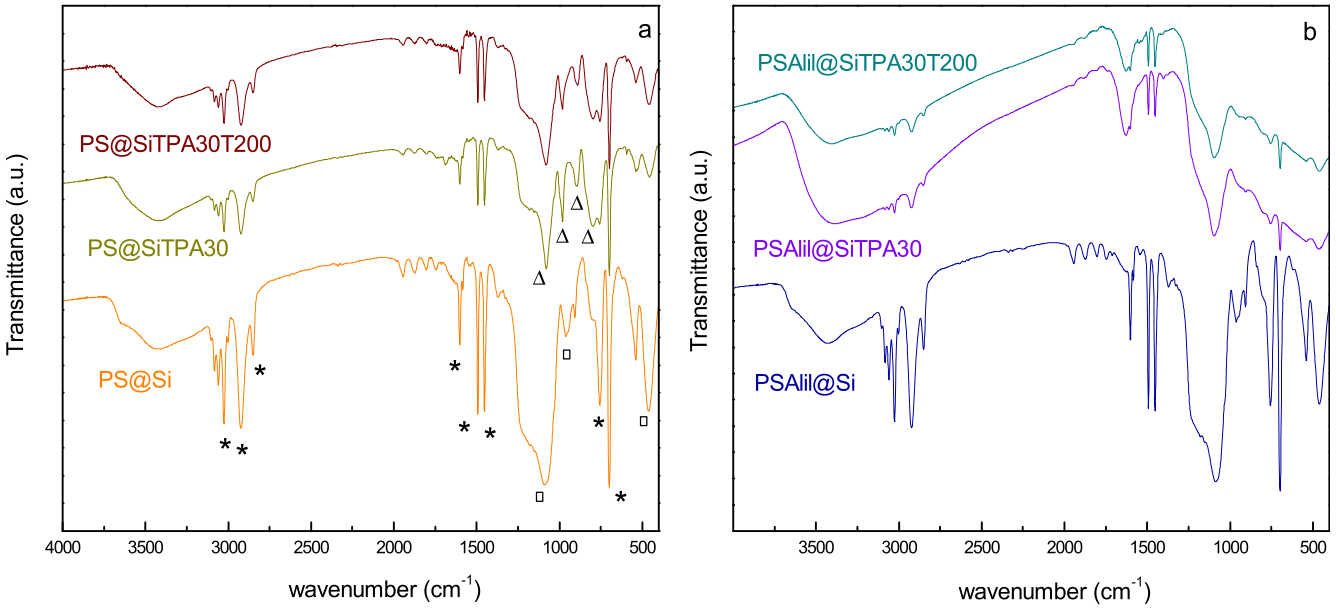

Fig. 5. FT-IR spectra of (a) PS@Si, PS@SiTPA30 and PS@SiTPA30T200 samples, (b) PSAlil@Si, PSAlil@SiTPA30 and PSAlil@SiTPA30T200 samples (main lines of PS (*), silica (□), TPA (Δ)).

Table 3
Textural properties of the materials.

Support	S_{BET} (m^2/g)	S_{Micro} (m^2/g)	V_p (cm^3/g)	V_{micro} (cm^3/g)	D_p (nm)
PS@Si	3	–	–	–	–
PS@SiTPA30	5	–	0.01	–	8.2
PS@SiTPA30T200	19	7	0.03	0.003	6.9
PSAlil@Si	14	–	0.03	0.003	6.8
PSAlil@SiTPA30	18	–	0.03	0.050	5.9
PSAlil@SiTPA30T200	22	5	0.02	–	5.3

consistent with those reported in the literature [30]. It must be remarked that Oa indicates oxygens bridging W placed in the four triads of the octahedra and the P heteroatom of the central tetrahedron that form the Keggin heteropolyanion primary structure, Ob corresponds to oxygens linking the triads through corners, Oc designates edge sharing oxygens, and Od denotes terminal oxygens [31].

For the materials prepared using allylamine as comonomer in the core (PSAlil@Si, PSAlil@SiTPA30 and PSAlil@SiTPA30T200 samples), all the spectra presented the characteristic bands of polystyrene, as in the case of the solids mentioned above. The bands assigned to the stretching vibrations of the bonds characteristic of the tungstophosphate anion and those of the comonomer are completely overlapped with the bands of the Si–O groups of silica, therefore they cannot be clearly visualized in the spectra. This fact may be probably due to a larger silica thickness layer than in the previously mentioned samples.

The textural properties of the prepared solids were determined through the N_2 adsorption–desorption isotherms at liquid N_2 temperature. The specific surface area (S_{BET}) of the materials, together with the mean pore diameter (Dp), estimated from the BET surface, and the total pore volume (Vp), estimated from the value corresponding to a $p/p_0 = 0.98$ ratio, as well as the specific micropore area (S_{Micro}) and the micropore volume (V_{micro}), both estimated from the t-plot method [32], are shown in Table 3.

For the material prepared by impregnation of the core/shell PS@Si solid (PS@SiTPA30 sample), it was observed that TPA addition did not lead to a significant modification of the specific surface area of the solid. When the PS@SiTPA30 solid is calcined at 200 °C, an increment of the S_{BET} value in the PS@SiTPA30T200 material is observed. This fact can be explained considering that, as a consequence of the heat treatment, the PS amount decreases and so, the Si/PS ratio increases; therefore the S_{BET} increment is due to the higher silica content in the material. On the other hand, for the material prepared by impregnating the PSAlil@Si solid with TPA (PSAlil@SiTPA30), the increase of the S_{BET} value is rather low. Additionally, its calcination did not cause an important increment either. This can be attributed to the fact that the PSAlil@SiTPA30 sample presents a higher shell/core ratio than the PS@SiTPA30 one, so the decrease of the PSAlil amount as a result of the thermal treatment is almost insignificant and the Si/PS ratio remains constant.

All the materials present mean pore diameter higher than 2 nm and, according to the IUPAC classification, correspond to mesoporous materials, with Vp notably higher than the micropore volume. The N_2 adsorption–desorption isotherms of the solids prepared using the core with comonomer addition are presented in Fig. 6. They are type IV isotherms and present type H2 hysteresis. Similar results were obtained for the other materials (PS@Si, PS@SiTPA30 and PS@SiTPA30T200 samples).

The TPA-impregnated solids were analyzed by ^{31}P MAS–NMR spectroscopy before and after calcination at 200 °C (Fig. 7). The spectrum corresponding to the PS@SiTPA30 sample displayed the peak with higher intensity placed at −15.5 ppm, which may be assigned to a TPA hydrated species, such as the $H_3PW_{12}O_{40}.6H_2O$ hydrate, in which the interaction that prevails is between the tungstophosphate anion and the protons associated with water. Another line is observed, placed at −15.0 ppm, which is attributed to an electrostatic interaction of TPA with the support such as $[H_{3-X}PW_{12}O_{40}]^{-X}$ $[H_2O–Si{=}]^{+}$ [33]. When the solid is calcined at 200 °C (PS@SiTPA30T200 sample), the reverse intensity ratio of the same lines is observed, the higher intensity peak assigned to the

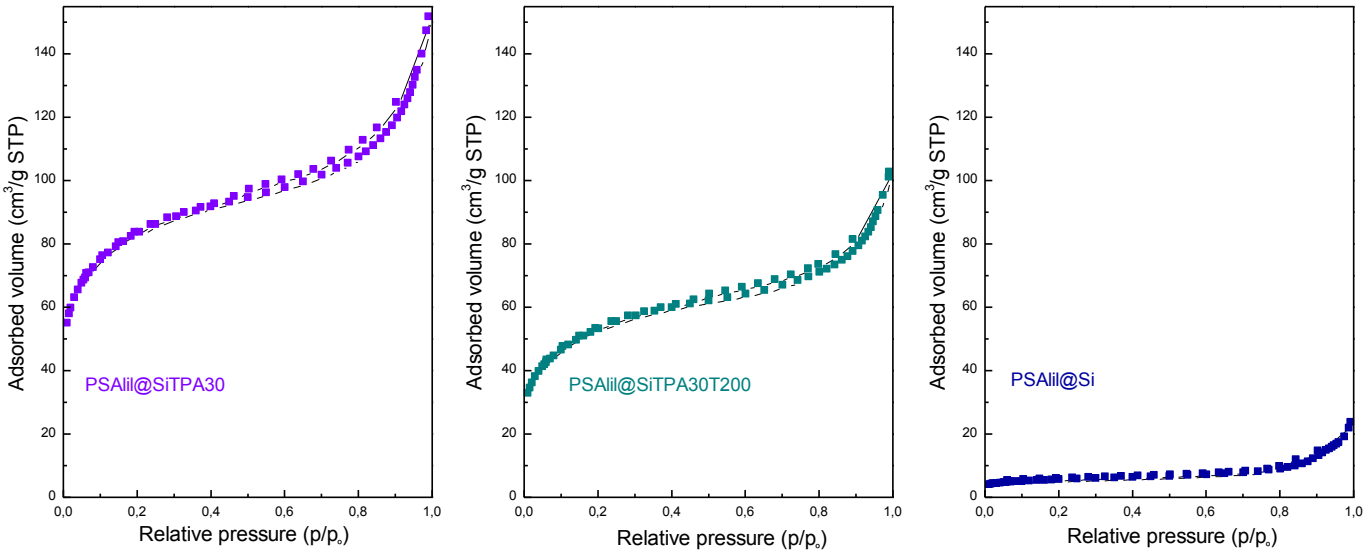

Fig. 6. Adsorption–desorption isotherms at liquid N_2 temperature of the PSAlil@Si, PSAlil@SiTPA30 and PSAlil@SiTPA30T200 solids.

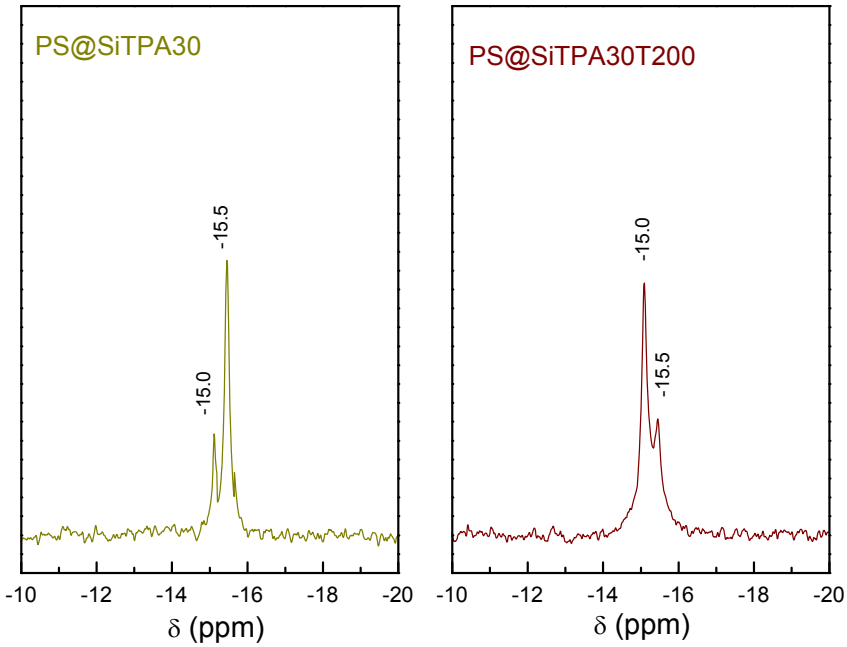

Fig. 7. ^{31}P MAS–NMR spectra of PS@SiTPA30 and PS@SiTPA30T200 samples.

interaction between tungstophosphate and the support being placed at −15.0 ppm, which may be attributed to the decrease in hydration degree of TPA when the solid is thermally treated. A similar behavior was detected for the PSAlil@SiTPA30 and PSAlil@SiTPA30T200 samples.

The XRD patterns of the PS@Si sample, the solid impregnated with TPA before (PS@SiTPA30 sample) and after calcination (PS@SiTPA30T200 sample) are shown in Fig. 8a. Peaks corresponding to crystalline phases appear in the solids impregnated with TPA, which are characteristic of the heteropolyacid, and may be present together with non-crystalline species interacting with the support. These results corroborate those obtained by FT-IR and NMR. A slight shifting of the lines is observed when the material is calcined at 200 °C.

The characteristics of the XRD patterns of the solids obtained using PS core with the addition of comonomer impregnated with TPA are similar to the pattern corresponding to the support; crystalline peaks are not observed (Fig. 8b). It may be inferred that the TPA species are well dispersed on the support as a non-crystalline form, or too small crystallites to be detected by this technique could be present.

The patterns of TPA with different hydration degrees are presented in Fig. 9. Here it can be observed that the PS@SiTPA30 sample presents a pattern with peaks at low angles and many other peaks overlapped with the broad bands of the support, which could be assigned to TPA with a high hydration degree because it

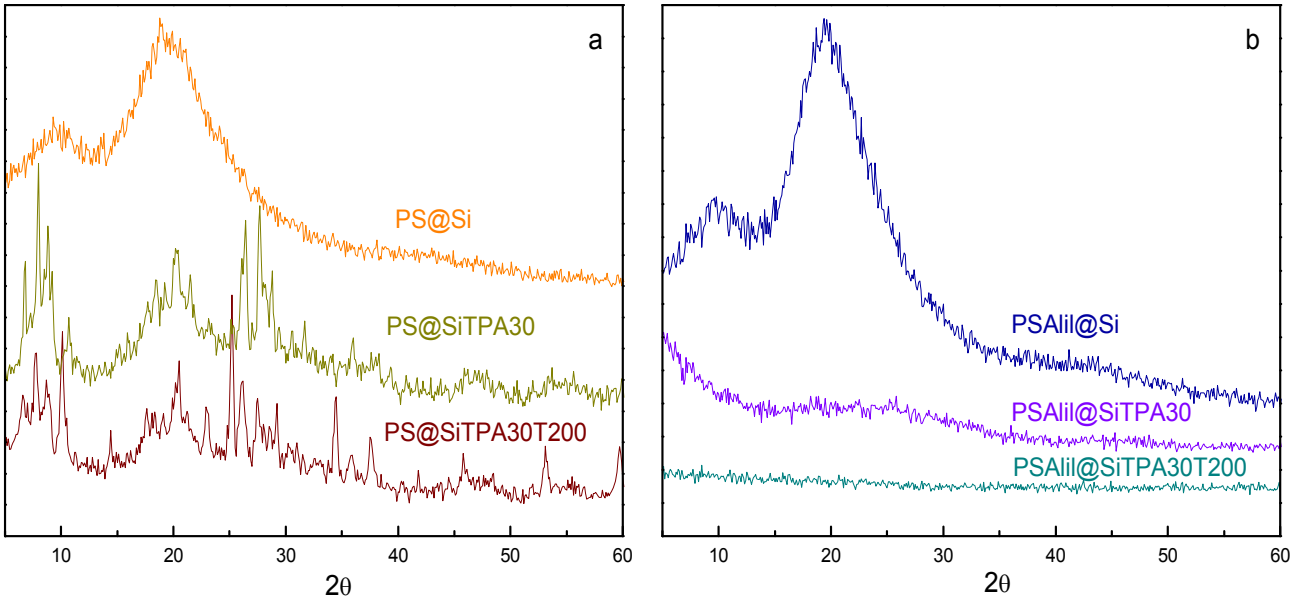

Fig. 8. XRD patterns of (a) PS@Si, PS@SiTPA30 and PS@SiTPA30T200 samples, (b) PSAlil@Si, PSAlil@SiTPA30 and PSAlil@SiTPA30T200 samples.

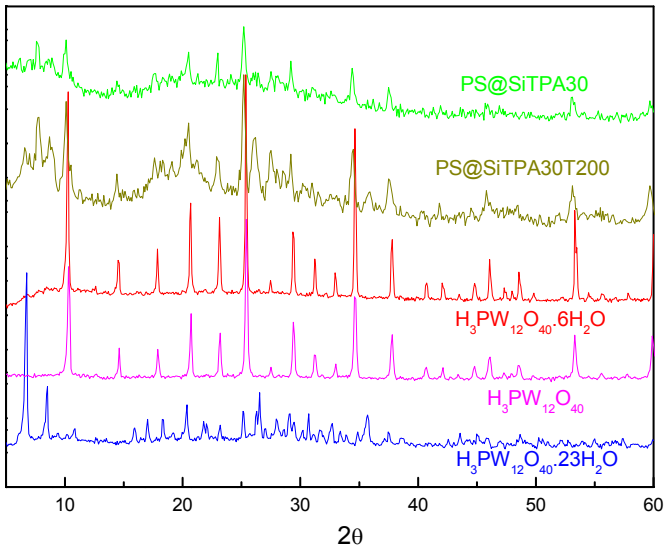

Fig. 9. XRD patterns of $H_3PW_{12}O_{40}.23H_2O$, $H_3PW_{12}O_{40}.6H_2O$, $H_3PW_{12}O_{40}$, PS@SiTPA30, and PS@SiTPA30T200 materials.

resembles the pattern of $H_3PW_{12}O_{40}.23H_2O$ material, though some peaks match well with those corresponding to the $H_3PW_{12}O_{40}.6H_2O$ solid. On the other hand, when this material is calcined at 200 °C (PS@SiTPA30T200 sample), the pattern presents characteristics more coincident with that of the $H_3PW_{12}O_{40}.6H_2O$ material, which could be due to water loss during calcination.

The strength and the number of acid sites present in the solids can be estimated by potentiometric titration with n-butylamine. It is considered that the initial electrode potential (Ei) indicates the maximum strength of the acid sites, and the value from which the plateau is obtained (meq amine/g solid) or the area under the curve accounts for the total number of acid sites that the titrated solid presents.

The strength of the acid sites can be classified according to the following scale: Ei > 100 mV (very strong sites), 0 < Ei < 100 mV (strong sites), −100 < Ei < 0 mV (weak sites), and Ei < 100 mV (very weak sites) [34].

From the potentiometric titration curves of the PS@SiTPA30, PS@SiTPA30T200 and PSAlil@SiTPA30, PSAlil@SiTPA30T200 solids, Ei values of 765, 461, 271, 231 mV, respectively, were measured (Fig. 10). So, it could be established that the materials present very strong acid sites, the solids prepared with the PS core being those having higher initial acid strength values. Although very strong acid sites were observed when the PS core with allylamine addition was employed, the Ei values were significantly lower.

As shown in Fig. 10a, the initial potential decreased when the solid was thermally treated at 200 °C, and the number of acid sites is lower because the plateau is reached at a lower n-butylamine amount and a lower area under the curve is observed for the PS@SiTPA30T200 sample compared to the PS@SiTPA30 material. A similar behavior was observed for the solids prepared with the PS core with allylamine addition, which are presented in Fig. 10b, because the potential and the number of acid sites decreased when the solid was thermally treated at 200 °C.

On the other hand, the titration curve of the supports presented potential values lower than those of the solids impregnated with TPA, due to the acidic characteristics of undegraded TPA. The Ei values obtained were 127 and 81 mV for PS@Si and PSAlil@Si samples, respectively.

In sum, core/shell materials appropriate to be used as support of catalytic compounds were prepared. The impregnation of these solids with tungstophosphoric acid allowed maintaining the Keggin structure of the acid, so leading to high acidic materials, suitable to be used in acid catalyzed reactions.

4. Conclusions

Polystyrene microspheres were obtained; their mean size was 1.0 or 2.5 μm according depending on whether the core was synthesized with 3-amino-1-propene or without the addition of this comonomer, respectively. It is clear that comonomer addition influenced the latex sphere size. The PS spheres were coated with a layer of silica nanoparticles with a smooth and uniform morphology. These characteristics were achieved using TEOS as silica precursor, NH_4OH as catalyst of the sol–gel reaction, and carefully controlling the temperature. A silica layer thickness of

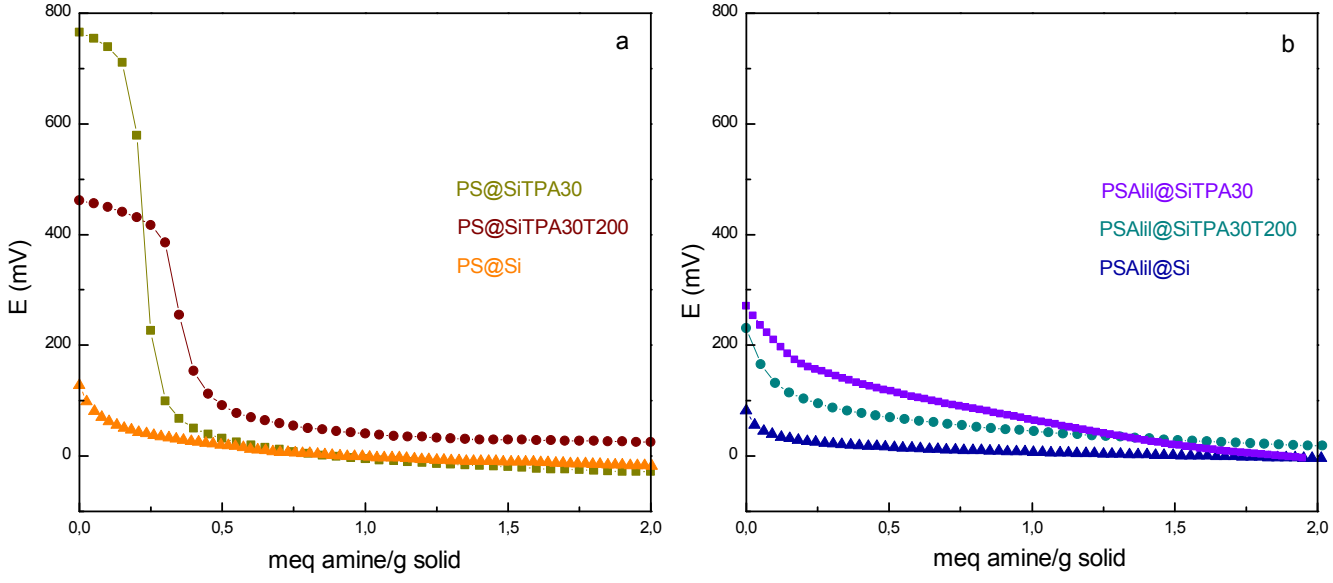

Fig. 10. Potentiometric titration curves of (a) PS@Si, PS@SiTPA30, and PS@SiTPA30T200 solids, (b) PSAlil@Si, PSAlil@SiTPA30 and PSAlil@SiTPA30T200 solids.

100 nm was obtained, as measured by TEM.

The FT-IR spectra of all the materials impregnated with TPA presented some characteristic bands of polystyrene even after calcination at 200 °C, so the material used as support contains moieties of the polymer. The bands assigned to the tungstophosphoric acid with undegraded Keggin structure were also present in all the solids. The materials without calcination presented a BET specific surface area lower than that of the solids calcined at 200 °C, and the impregnation with TPA in the different supports increased these values. On the other hand, the potentiometric titration of all the impregnated solids showed that the materials have very strong acid sites.

All the results indicate that the prepared materials are good candidates to be used in reactions catalyzed by acids, such as imidazole synthesis, which is the reaction in which they will be applied.

Acknowledgments

The authors thank the experimental contribution of E. Soto, G. Valle, M. Theiller, L. Osiglio and M. Baez, and the financial support of CONICET and UNLP.

References

[1] S. Wang, M. Zhang, D. Wang, W. Zhang, S. Liu, Micropor. Mesopor. Mater 139 (2011) 1–7.
[2] R. Hayes, A. Ahmed, T. Edge, H. Zhang, J. Chromatogr. A 1357 (2014) 36–52.
[3] W. Li, D. Zhao, Adv. Mater. 25 (2013) 142–149.
[4] R.G. Chaudhuri, S. Paria, Chem. Rev. 112 (2012) 2373–2433.
[5] K.T. Li, M.H. Hsu, I. Wang, Catal. Commun. 9 (2008) 2257–2260.
[6] C. Wu, X. Sun, Z. Zhao, Y. Zhao, Y. Hao, Y. Liu, Y. Gao, Mater. Sci. Eng. C 44 (2014) 262–267.
[7] J.D. Rocca, D. Liu, W. Lin, Acc. Chem. Res. 44 (2011) 957–968.
[8] J.J. DeStefano, S.A. Schuster, J.M. Lawhorn, J.J. Kirkland, J. Chromatogr. A 1258 (2012) 76–83.
[9] L.E. Blue, J.W. Jorgenson, J. Chromatogr. A 1218 (2011) 7989–7995.
[10] H. Fan, Z. Lei, J.H. Pan, X.S. Zhao, Mater. Lett. 65 (2011) 1811–1814.
[11] I. Tissot, J.P. Reymond, F. Lefebvre, E. Bourgeat-Lami, Chem. Mater. 14 (2002) 1325–1331.
[12] J. Yang, J.U. Lind, W.C. Trogler, Chem. Mater. 20 (2008) 2875–2877.
[13] K. Zhang, X. Zhang, H. Chen, X. Chen, L. Zheng, J. Zhang, B. Yang, Langmuir 20 (2004) 11312–11314.
[14] X. Liu, H. Wu, F. Ren, G. Qiu, M. Tang, Mater. Chem. Phys. 109 (2008) 5–9.
[15] L.R. Pizzio, P.G. Vázquez, C.V. Cáceres, M.N. Blanco, Appl. Catal. A General 256 (2003) 125–139.
[16] I.V. Kozhevnikov, Chem. Rev. 98 (1998) 171–198.
[17] V.D. Monopoli, L.R. Pizzio, M.N. Blanco, Mater. Chem. Phys. 108 (2008) 331–336.
[18] V. Fuchs, L. Méndez, M. Blanco, L. Pizzio, Appl. Catal. A General 358 (2009) 73–78.
[19] T.S. Rivera, A. Sosa, G.P. Romanelli, M.N. Blanco, L.R. Pizzio, Appl. Catal. A General 443–444 (2012) 207–213.
[20] A. Sosa, T.S. Rivera, M.N. Blanco, L.R. Pizzio, G.P. Romanelli, Phosphorus Sulfur Silicon Relat. Elem. 188 (2013) 1071–1079.
[21] L.R. Pizzio, C.V. Cáceres, M.N. Blanco, Appl. Surf. Sci. 151 (1999) 91–101.
[22] D. Bennardi, G. Romanelli, J. Autino, L. Pizzio, P. Vázquez, C. Cáceres, M. Blanco, Reac. Kinet. Mech. Cat. 100 (2010) 165–174.
[23] W. Stöber, A. Fink, E. Bohn, J. Colloid Interface Sci. 26 (1968) 62–69.
[24] M. Gorsd, M.N. Blanco, L.R. Pizzio, Procedia Mater. Sci. 1 (2012) 432–438.
[25] O.H. Kim, K. Lee, K. Kim, B.H. Lee, S. Choe, Polymer 47 (2006) 1953–1959.
[26] H. Zou, S. Wu, J. Shen, Langmuir 24 (2008) 10453–10461.
[27] M. Gorsd, L.R. Pizzio, M.N. Blanco, Procedia Mater. Sci. 8 (2015) 567–576.
[28] K. Zhang, W.L. Zhang, H.J. Choi, Colloid Polym. Sci. 291 (2013) 955–962.
[29] C.J. Pouchert (Ed.), The Aldrich Library of Infrared Spectra, Edition III, Aldrich Chemical Co., 1981.
[30] C. Rocchiccioli-Deltcheff, R. Thouvenot, R. Franck, Spectrochim. Acta A 32 (1976) 587–597.
[31] L.R. Pizzio, M.N. Blanco, Appl. Catal. A General 255 (2003) 265–277.
[32] R.Sh Mikhail, S. Brunauer, E.E. Bodor, J. Colloid Interface Sci. 26 (1968) 45–53.
[33] F. Lefebvre, J. Chem. Soc. Chem. Commun. (1992) 756–757.
[34] L. Pizzio, P. Vázquez, C. Cáceres, M. Blanco, Catal. Lett. 77 (2001) 233–239.